

Sexually dimorphic development of depression-related brain networks during healthy human adolescence

Dorfschmidt, L.^{1,*}, Bethlehem, R.A.I.¹, Seidlitz, J.², Váša, F.³, White, S.R.¹, Romero-García, R.¹, Kitzbichler, M.G.¹, Aruldass, A.¹, Morgan, S.E.^{1,11}, Goodyer, I.M.¹, Fonagy, P.⁷, Jones, P.B.^{1,6}, Dolan, R.J.^{4,5}, the NSPN consortium**, Harrison, N.A.^{8,9}, Vértes, P.E.^{1,10,11}, and Bullmore, E.T.^{1,6}

¹ Department of Psychiatry, University of Cambridge, Cambridge, CB2 0SZ, UK

² Department of Psychiatry, University of Pennsylvania, Philadelphia, PA 19104, USA

³ Department of Neuroimaging, King's College London, SE5 8AF, UK

⁴ Wellcome Trust Centre for Neuroimaging, University College London Institute of Neurology, University College London, London WC1N 3BG, UK

⁵ Max Planck University College London Centre for Computational Psychiatry and Ageing Research, University College London, London WC1B 5EH, UK

⁶ Cambridgeshire and Peterborough NHS Foundation Trust, Huntingdon, PE29 3RJ, UK

⁷ Research Department of Clinical, Educational and Health Psychology, University College London, London WC1E 6BT, United Kingdom

⁸ Department of Neuroscience, Brighton and Sussex Medical School, University of Sussex Campus, Brighton, BN1 9RY, UK

⁹ Cardiff University Brain Research Imaging Centre, Cardiff University, Cardiff, CF24 4HQ, UK

¹⁰ School of Mathematical Sciences, Queen Mary University of London, London E1 4NS, UK

¹¹ The Alan Turing Institute, London NW1 2DB, UK

** A complete list of the NSPN Consortium can be found in the SI Appendix.

*Corresponding author. ld548@cam.ac.uk

24/7/2020

Abstract Adolescence is a period of critical development of the brain, that coincides with a sexually dimorphic increase in risk of depression for females. We hypothesized that there might be sexual dimorphisms in human brain network development underlying the dimorphism in depression. First, we tested for sex differences in parameters of brain network development (baseline connectivity at age 14, FC_{14} , adolescent change in connectivity FC_{14-26} , and maturational index, MI), measured repeatedly in resting state functional MRI scans from $N=298$ healthy young people aged 14-26 years, scanned a total of 520 times. We measured the maturational index ($-1 < MI < 1$) at each of 346 regions for each sex separately. Regions with negative MI were located in the cortical default mode network (DMN), the limbic system and subcortical nuclei. This cortico-subcortical system shared a disruptive pattern of development, e.g., weak functional connectivity with these regions at age 14 became stronger over the course of adolescence. This developmentally disruptive system was sexually dimorphic, i.e., the sex difference in MI was significantly less than zero at 83 regions. We then investigated the biological plausibility, and relevance to depression, of this fMRI-derived map of dimorphic brain development. It was significantly co-located with the cortical expression map of a weighted function of whole genome transcription, by partial least squares regression on prior adult post mortem data. Genes that were most strongly expressed in disruptively developing brain regions were enriched for X chromosome genes; genes specialized for perinatal and adolescent phases of cortical and subcortical development, respectively; and risk genes for major depressive disorder (MDD), defined by genome-wide significant association. The dimorphic development map was also significantly co-located with (i) brain regions activated by prior task-activated fMRI studies of reward and emotional processing and (ii) a map of adult MDD-related differences in functional connectivity from an independent case-control fMRI study ($N=96$). We conclude that sex differences in adolescent development of cortico-subcortical functional network connectivity were biologically validated by anatomical co-location with brain tissue expression of sex-, development- and MDD-related genes. Dimorphically disruptive development of DMN, limbic and subcortical connectivity could be relevant to the increased risk of depressive symptoms in adolescent females.

¹ Introduction

² Adolescence is a period of critical development of the brain, characterized by changes in both structure (1; 2; 3; 4) and function (5; 6), that coincide with changes in cognition and behaviour. It is also a time of increasing incidence of many psychiatric disorders,

including depression, which occurs more frequently in females than males (7; 8). Small sex differences in mood have been reported from the age of 11, and by the age of 15 females are about twice as likely to be depressed as males (7; 8; 9). Recent work has supported the idea that sexually-dimorphic risk for mood disorders

Statistic	Sex	Age Stratification					All Ages
		14-15	16-17	18-19	20-21	22-25	
N Subjects	Female	34	39	24	32	22	151
	Male	32	33	24	35	23	147
FD, mm	Female	0.13*	0.10*	0.12	0.10	0.13	0.11*
	Male	0.15*	0.13*	0.12	0.14	0.13	0.13*
N Scans/Subject (1 2 3)	Female	9 22 3	11 25 3	6 16 2	14 16 2	14 7 1	54 86 11
	Male	7 24 1	8 24 1	7 16 1	11 20 4	8 14 1	41 98 8

* $P_{uncorr.} < 0.05$

Table 1 Adolescent developmental MRI sample. Total N = 298 healthy young people participated in an accelerated longitudinal MRI study, with recruitment balanced for sex in each of five age-defined strata, and each participant scanned at least twice (baseline and follow-up 18 months later). FD = framewise displacement, a measure of head movement in mm, was significantly greater in males compared to females on average over all ages, and in the youngest two age strata specifically ($P < 0.05$, uncorrected)(SI Fig. S1).

11 could be related to sex-dimorphisms in adolescent brain network
12 development (10).

13 Functional brain networks derived from resting state functional
14 magnetic resonance imaging (rs-fMRI) can be used to study
15 complex network organization in the brain. Each node of these net-
16 works is an anatomical region and each edge weight is an estimator
17 of association, so-called functional connectivity, typically the cor-
18 relation or coherence between the two fMRI signals simultaneously
19 measured for each possible pair of nodes in the network (11; 12).

20 The brain is plastic and undergoes maturational changes
21 throughout life. Previous resting-state fMRI studies have sug-
22 gested that during adolescence a shift from local to distributed
23 networks (13) and an increase in the strength of long-range connec-
24 tions (14; 15) occurs. Since most long-range connections originate
25 from association cortical areas, these maturational processes have
26 previously been associated with the idea that primary sensory and
27 motor areas mature most rapidly during childhood, while associa-
28 tion areas undergo their most profound changes during late adoles-
29 cence (6; 16; 17). However, it has since been noted that in-scanner
30 head motion may have confounded many of the effects previously
31 attributed to age, particularly in younger participants (18; 19; 20).
32 Developmental imaging studies have therefore employed different
33 strategies to address these concerns, e.g., by restricting analysis
34 to motion-uncontaminated sub-samples of acquired data with no
35 detectable head motion (6), or by regressing each nodal fMRI
36 signal on the global average fMRI signal (21). Issues concerning
37 optimal head motion correction for pre-processing fMRI data
38 remain controversial (22; 23; 24).

39 It is not yet clear how functional connectivity differs between
40 males and females, either during adolescence or adulthood. One
41 widely reported sex difference is increased functional connectivity
42 of the default mode network (DMN) in females (25; 26; 27; 28; 29).
43 Female-increased connectivity has also been reported in the sub-
44 cortex and limbic areas (cingulate gyrus, amygdala, hippocampus)
45 (30); whereas male-increased connectivity has been reported for
46 sensori-motor areas (30; 25; 28). However, these effects are not
47 consistently found across studies (27; 26; 31). Importantly, most
48 research on sex differences has focused on pre-selected regions,
49 often including the amygdala (32; 33), with few studies having
50 investigated sex differences comprehensively over all brain regions

51 (25; 28; 34; 35; 36). Most prior fMRI studies of brain development
52 have focused on estimating "average" effects of age across both
53 sexes, e.g., by including sex as a covariate in the statistical model
54 for estimation of developmental parameters (cf. Table 4 in Supple-
55 mentary Materials) and few have reported age-by-sex interactions
56 or the conditioning of developmental parameters by sex (35; 30).

57 We start from the hypothesis that the sexually dimorphic risk
58 trajectory for depression, with higher depressive symptom scores
59 for adolescent females than males (7; 8), could be the psycho-
60 logical or clinical representation of an underlying dimorphism in
61 adolescent brain network development (34; 27; 28).

62 To investigate this overarching hypothesis experimentally, we
63 first identified sexually dimorphic systems of healthy adolescent
64 brain development, and then tested the anatomical co-location of
65 dimorphic fMRI systems with prior maps of human brain gene
66 expression and depression-related fMRI phenotypes.

67 We estimated the effects of sex on three parameters of ado-
68 lessent development of resting-state functional connectivity, using
69 fMRI data from an accelerated longitudinal study (N=298; age
70 range 14-26 years; 50% female; Table 1), stratified by age and
71 balanced for sex per age stratum (37). There was a significant sex
72 difference in head motion (framewise displacement, FD, mm) dur-
73 ing fMRI scanning, so we pre-processed the data to mitigate the
74 potentially confounding effects of head motion and subsequently
75 demonstrated the robustness of the key results to alternative
76 fMRI pre-processing strategies. We found that females had sig-
77 nificantly more disruptive development of functional connectivity
78 in a default mode cortical, limbic and subcortical network. We
79 then tested the hypotheses that this developmentally dimorphic
80 brain system was co-located with expression of a weighted func-
81 tion of the whole genome enriched for X chromosome genes, genes
82 related to perinatal and post-natal brain development, and genes
83 related to major depressive disorder (MDD). We also tested the
84 hypothesis that the sexually dimorphic system was co-located with
85 an anatomical map of depression-related differences in func-
86 tional connectivity from an independent case-control fMRI study
87 of MDD.

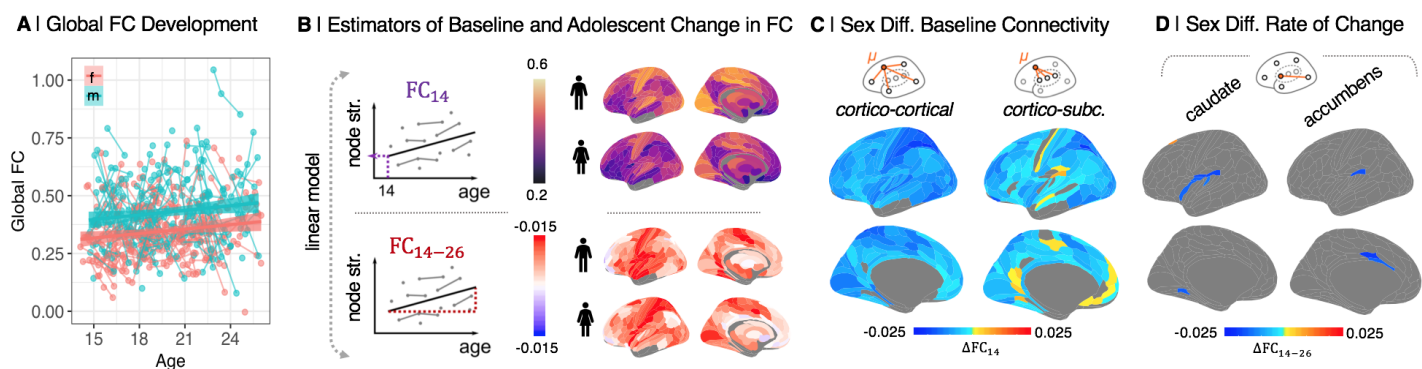


Fig. 1 Sex differences in functional connectivity at age 14 (FC_{14}) and adolescent rate of change of connectivity (FC_{14-26}): (A) Global functional connectivity (FC) strength increased with age ($t(219)=2.3, P<0.05$) and was higher in males ($t(296)=5.5, P<0.0001$). (B) To estimate two parameters of development at each regional node, we fit a linear model to the relationship between age and weighted degree (k , nodal strength of connectivity to the rest of the network) for males and females separately. The two model parameters are the intercept, or "baseline" connectivity at age 14 (FC_{14}), and the linear rate of change in connectivity during adolescence (FC_{14-26}). (C) We found 323 regions had significantly increased cortico-cortical connectivity, and 309 regions had increased cortico-subcortical connectivity ($P_{FDR}<0.05$; 95.7%), at baseline, FC_{14} , in males. (D) FC_{14-26} was only significantly different between sexes, decreased in females, in subcortico-cortical connectivity of the caudate and nucleus accumbens.

88 Results

89 Analysable sample and head motion

90 A total of 36 scans were excluded by quality control criteria
91 including high in-scanner motion (mean FD > 0.3 mm or maximum
92 FD>1.3 mm), co-registration errors, or low variance due to
93 widespread susceptibility artefacts. The analyzable sample thus
94 consisted of 520 scans from 298 participants (151 females; Table
95 1, Fig. S1). Males had significantly more head movement than
96 females in the youngest two age strata ($P<0.05$, uncorrected) and
97 on average over all ages (Table 1).

98 After pre-processing for within-subject correction of head
99 motion effects on individual fMRI time series, functional connec-
100 tivity was positively correlated with individual differences in
101 mean FD, and this effect scaled with distance between the nodes
102 (SI Fig. S2A). We therefore also corrected for between-subject
103 differences in head motion by regressing each inter-regional cor-
104 relation on mean FD across all participants. This removed the
105 relationship between connectivity and FD, as well as the distance-
106 dependence in this relationship (18; 38) (SI Fig. S2). To assess the
107 robustness of key results to this two-step process for head motion
108 correction, we conducted three sensitivity analyses: (i) sex-specific
109 motion correction - FC matrices were regressed on FD separately
110 for males and females (SI Text, SI Fig. S24-27); (ii) GSR cor-
111 rection - the fMRI time series at each node were regressed on
112 the global fMRI signal per participant (SI Text, SI Fig. S21-23);
113 and (iii) motion-matched sub-sample analysis - we used a subset
114 of data ($N=314$), comprising equal numbers of males and females,
115 for which there was no statistical difference in FD (SI Text, SI Fig.
116 S17-20). There was a significant correlation between the develop-
117 mental parameters (FC_{14} , FC_{14-26} , and MI) estimated by each of
118 these alternative head motion correction methods and the param-
119 eters estimated by our principal method (SI Fig. S28-29). The key

finding of dimorphic adolescent development of functional connec-
120 tivity between DMN, limbic and subcortical regions, as reported
121 below, was conserved in all cases.

122 Age and sex effects on functional connectivity

123 We modeled age and sex effects on global functional connectivity of
124 each participant, estimated as mean weighted degree, using linear
125 mixed effects models (LMEs). Functional connectivity increased
126 with age ($t(219)=2.3, P<0.05$) and males had higher global mean
127 connectivity degree than females ($t(296)=5.5, P<0.0001$) (Fig.
128 1A).

129 Sex differences in parameters of adolescent development

130 Regional functional connectivity was estimated between and
131 within cortical and subcortical subsets of nodes by averaging the
132 relevant parts of the connectivity matrix (SI Fig S3). To model
133 development of functional connectivity during adolescence, we
134 focused on three parameters: regional baseline connectivity at age
135 14, FC_{14} ; regional linear change in connectivity between 14-26
136 years, FC_{14-26} (Fig. 1B); and the signed Spearman correlation of
137 these two parameters (estimated at the edge-level), termed
138 maturational index ($-1 < MI < +1$) (Fig. 2A; (6)). Previous work
139 on this sample has reported developmental change (controlling for
140 sex) in terms of these parameters estimated at each regional node
141 of a whole brain fMRI network (6). Here we estimated each of these
142 parameters for males and females separately, and the between-sex
143 difference for each parameter, e.g., $\Delta MI = MI_{female} - MI_{male}$. We
144 tested the significance of the between-sex difference in each
145 parameter at each regional node using permutation or parametric
146 tests (SI Fig. S3, SI Text).

147 *Baseline connectivity at age 14* was greater in primary sen-
148 sorimotor cortex than in association cortex for both sexes (Fig.
149 1B, SI Fig. S4-5). As predicted by the sex difference in global
150 functional connectivity at all ages (Fig. 1A), males had signifi-
151 cantly stronger baseline connectivity than females at 14 years,

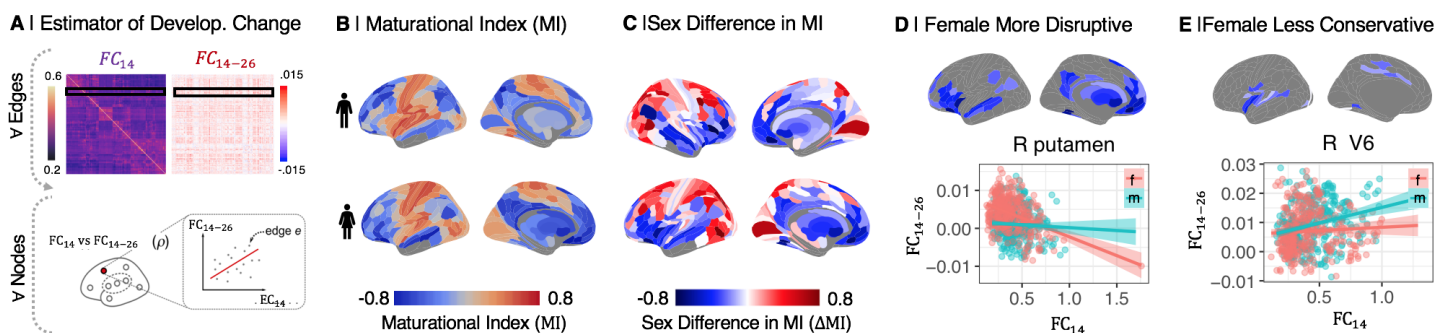


Fig. 2 Sex differences in maturational index (MI): (A) The maturational index (MI) was estimated as the correlation between edgewise baseline connectivity at age 14 (FC_{14}), and the adolescent rate of change in connectivity (FC_{14-26}), at each regional node. (B) MI maps for males and females separately. MI was generally negative (blue) in frontal and association cortical areas, and positive (orange) in primary motor and sensory cortices. (C) The sex difference in MI, $\Delta MI = MI_{female} - MI_{male}$, was significant in 230 regional nodes ($P_{FDR} = 0.05$). ΔMI was significantly negative (less than zero) in the ventral and medial prefrontal gyrus, ventrolateral prefrontal cortex, anterior and posterior cingulate gyrus, medial temporal gyrus, and subcortical nuclei (SI Table S2), indicating sex differences in adolescent development of connectivity of these regions. More specifically, negative ΔMI defined a set of brain regions where adolescent development was either more disruptive (weak connections at 14 years became stronger during adolescence, or strong connections became weaker) or less conservative (strong connections at 14 years became weaker during adolescence) in females compared to males. (D) Map of brain regions where development was more disruptive in females. As exemplified by right putamen, functional connections of disruptively developing nodes that were strong at 14 years (high FC_{14} , x-axis) became weaker over the period 14–26 years ($FC_{14-26} < 0$, y-axis), and edges that were weakly connected at 14 y became stronger over the course of adolescence, especially in females. (E) Map of brain regions where development was less conservative in females. As exemplified by right visual area V6, connections that were strong at baseline became stronger over the period 14–26 years, especially in males.

i.e., $\Delta FC_{14} = FC_{14,female} - FC_{14,male} > 0$, in cortico-cortical and cortico-subcortical connections, but not subcortico-cortical connections (Fig. 1C).

Adolescent rate of change in connectivity was strongly positive in sensorimotor cortex, and less positive or slightly negative in association cortical and limbic areas, for both sexes. There was no significant sex difference, i.e., $\Delta FC_{14-26} = 0$, for cortico-cortical and cortico-subcortical connectivity, but a subset of subcortico-cortical connections (involving caudate and nucleus accumbens) had significantly more negative rates of change in females compared to males (Fig. 1D, Fig. S8–S9; $P_{FDR} < 0.05$).

Maturational index was positive in sensorimotor cortex, and negative in association cortex and subcortical areas, in both sexes separately (Fig. 2B), as previously reported for both sexes on average (6). However, there were many areas of significant sex difference in MI ($P_{FDR} < 0.05$). Females had more negative MI than males in 107 regions (Fig. 2B; SI Table S2, SI Fig S11). In 84 of these regions, exemplified by the right putamen (Fig. 2D), there was more disruptive development in females, i.e., weak connections at 14 years became stronger during adolescence, or strong connections became weaker, in females compared to males. In 23 regions, exemplified by right visual area V6 (Fig. 2D), there was less conservative development in females, i.e., strong connections at 14 years became stronger during adolescence in males compared to females.

The unthresholded map of ΔMI was co-registered with a prior map of cortical cytoarchitectonic classes (Fig. 3B) and a prior map of resting state networks (39) from an independent component analysis of adult fMRI data (Fig. 3C). Regions of negative ΔMI were concentrated in secondary sensory, limbic, and insular

classes of cortex, and in subcortical structures, defined anatomically (Fig. 3B); and in default mode, limbic, ventral attentional and subcortical systems defined functionally (Fig. 3C).

Automated meta-analytic referencing of the unthresholded map of significantly negative ΔMI was conducted using the Neurosynth database of task-related fMRI activation coordinates (40). This indicated that regions with more disruptive (or less conservative) development in females were typically activated by tasks related to reward processing, emotion, motivation, incentive delay, and dopamine (Fig. 3C).

Gene transcriptional enrichment of dimorphically developing brain systems

To investigate the relationships between gene transcriptional profiles and sexually dimorphic adolescent brain development, we used partial least squares (PLS) regression to find the weighted gene expression pattern that was most closely co-located with the ΔMI map (Fig. 3A; (5; 42)). Whole genome transcripts were estimated for the average of each of 180 bilaterally homologous cortical regions using adult post-mortem data ($N=6$) provided by the Allen Human Brain Atlas (27).

The first PLS component (PLS1; Fig. 3A) explained 34.6% of the variance in ΔMI , significantly more than expected by chance ($P_{perm.} < 0.05$). The PLS1 gene expression weights were positively correlated with ΔMI , thus negatively weighted genes were over-expressed in regions with negative ΔMI , and positively weighted genes were under-expressed in regions of negative ΔMI (Fig. 4B). To test the hypothesis that sex chromosomal gene expression was related to the sexual dimorphism in adolescent brain development, we assessed chromosomal enrichment of the genes on PLS1. We found that the most negatively weighted genes, which were highly expressed in disruptively developing regions, were most strongly

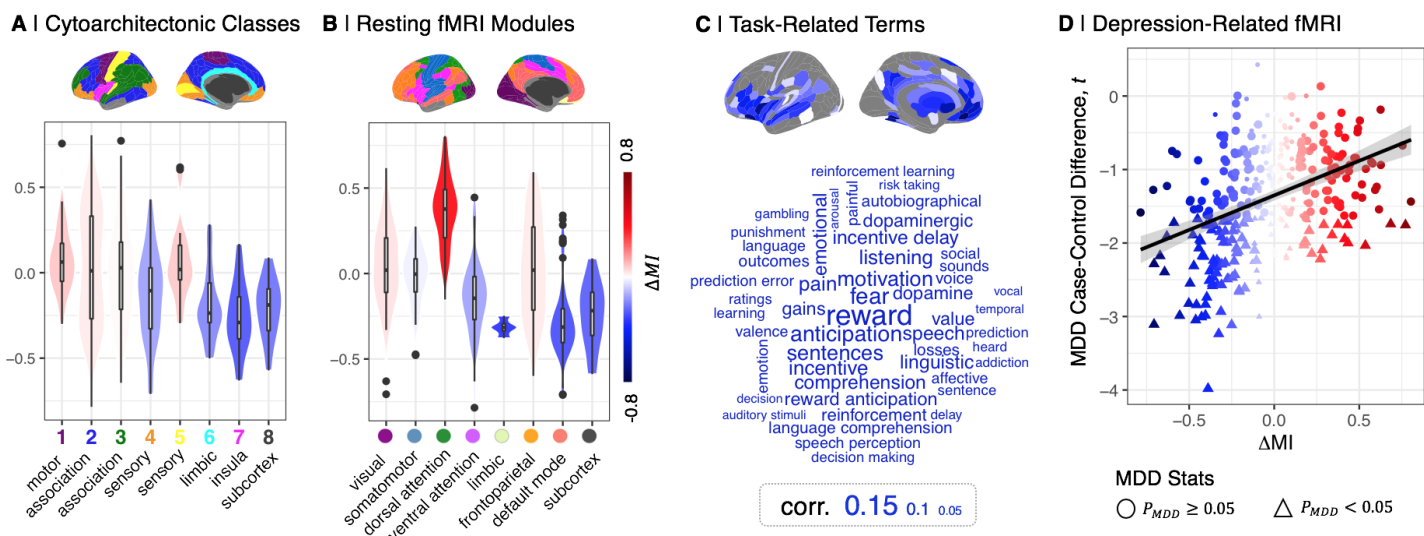


Fig. 3 Sex difference in maturational index in psychological and psychiatric context: (A) ΔMI was most negative in secondary sensory, limbic, and insula cortex, and subcortical structures defined by cell type, (B) as well as functionally defined default mode network (DMN), ventral attention network, limbic, and subcortical structures. (C) Wordcloud of Neurosynth meta-analytical cognitive terms scaled according to their strength of association with the disruptively developing brain regions (cortical map of $\Delta MI < 0$). (D) Top, identically parcellated brain map of MDD case-control differences in weighted degree, t statistics. Bottom, ΔMI (x-axis) was positively correlated with case-control t -statistics (y-axis; $\rho = 0.4$, $P < 0.001$). Regions with dimorphically disruptive development in adolescence (negative ΔMI) had reduced degree of connectivity in adult MDD cases.

enriched for X chromosome genes ($P < 0.001$; Fig. 4C, SI Table S4). Regional differences in cortical gene expression have been attributed to different proportions of functionally specialised neuronal, glial and other cell types in different cortical areas (43). We therefore used the Cell Specific Enrichment Analysis tool (CSEA) tool (44) to assess cell type enrichment of the most positively and negatively weighted genes on PLS1. We found that negatively weighted genes ($Z < -2.58$) were enriched for genes with cortical expression in late fetal and early postnatal life, and for genes with amygdala, hippocampal and striatal expression in late childhood and adolescence (Fig. 4D). In contrast, positively weighted genes ($Z > 2.58$) were enriched for genes with cortical, cerebellar and thalamic expression during adolescence and young adulthood (Fig. 4D). This result indicates that the negatively weighted genes, most strongly co-expressed with the disruptively developing cortico-subcortical system, were specialised for perinatal and adolescent phases of cortical and subcortical development, respectively. We further explored developmental aspects of the sexually dimorphic system by testing for enrichment by genes specific to pre-natal and post-natal cell types (45). We found that genes which were over-expressed in disruptively developing brain regions were enriched for pre-natal cell types (46), including oligodendroglial precursor cells (OPC), microglia, astrocyte progenitor radial cells, inhibitory and excitatory cortical neurons (Fig. 4E), as well as for multiple adult glial and neuronal cell classes (Fig. 4F, SI Fig. S14).

Dimorphic brain development and depression

Extending the enrichment analysis to consider depression-related genes, we found that the list of genes strongly co-expressed with dimorphically disruptive brain systems was significantly enriched

for genes with genome-wide association with major depressive disorder (MDD) (41). Specifically, the MDD risk genes were negatively weighted and ranked towards the bottom of the PLS1 list, indicating that they were more highly-expressed in brain regions with disruptive development, indexed by negative ΔMI .

To assess the anatomical correspondence between the dimorphically disruptive brain system, and mood disorder-related changes in fMRI connectivity, we used resting state fMRI data from a prior case-control study of adult MDD cases ($N=50$) and healthy controls ($N=46$); see (SI Table S3). The parcellated, unthresholded map of MDD case-control differences in weighted degree (comprising 346 regional t statistics), was significantly co-located with the identically parcellated, unthresholded map of ΔMI ($\rho = 0.4$, $P < 0.001$; Fig. 3D). Brain regions with sexually dimorphic development in adolescence (negative ΔMI) had reduced degree of functional connectivity in MDD cases compared to controls.

Discussion

In this accelerated longitudinal fMRI study of healthy young people, we have identified human brain systems that demonstrated a significantly different pattern of adolescent development in females compared to males. We found sex differences in several aspects of functional connectivity (FC): females had lower global mean FC across all ages, and reduced nodal strength of connectivity in most regional nodes at 14 years FC_{14} . However, there were more anatomically specific sex differences in two developmentally sensitive parameters: the rate of change in FC during adolescence, FC_{14-26} , was significantly reduced in females for connections between subcortical and cortical structures; and the maturational

243
244
245
246
247
248
249
250
251
252
253
254
255
256
257
258
259
260
261
262
263
264
265
266
267
268
269
270

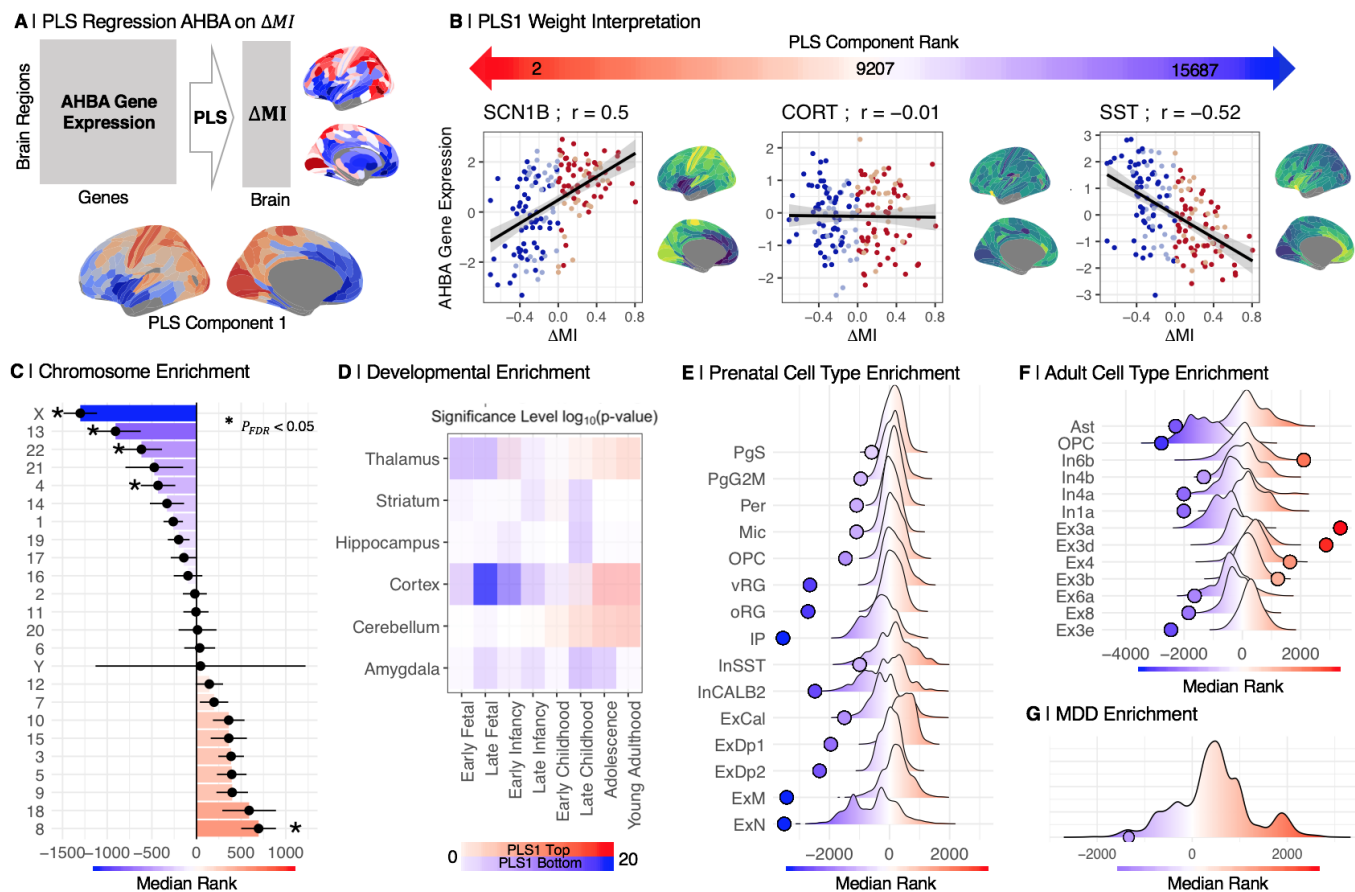


Fig. 4 Dimorphically disruptive brain systems are co-located with brain tissue transcripts enriched for X chromosome, neurodevelopmental, and MDD risk genes: (A) We used partial least squares (PLS) regression to map the Allen Human Brain Atlas (AHBA) gene expression data (27) onto the ΔMI map. (B) Relationship of ΔMI to expression of exemplary single genes: *SCN1B*, a positively weighted gene close to the top of the ranked list of PLS1 weights; *CORT*, a near-zero weighted gene in the middle of the list; and *SST*, a negatively weighted gene close to the bottom. Negatively weighted genes were more strongly expressed in regions with more disruptive development in females indicated by negative ΔMI ; whereas positively weighted genes were more strongly expressed in regions with female more conservative development indicated by positive ΔMI . (C) Enrichment analysis for chromosomal genes. Plot of the median rank of genes from each chromosome on PLS1, with standard deviations. (D) Enrichment analysis for neurodevelopmental genes. Negatively weighted genes (blue) were enriched for genes typically expressed in cortex during late fetal and early post-natal development and for genes expressed in the amygdala, hippocampus and striatum during late childhood and adolescence. Positively weighted genes (red) were enriched for genes typically expressed in cortex and cerebellum during adolescence and early adult life. (E) Enrichment analysis for prenatal cell type-specific genes. Negatively weighted genes (blue) were significantly enriched for genes expressed by prenatal radial glia (vRG, oRG), microglia (Mic), oligodendrocyte progenitor cells (OPC), and excitatory neurons. (F) Enrichment analysis for adult cell type-specific genes. Negatively weighted genes were significantly enriched for genes expressed by adult astrocytes, OPC, and excitatory neurons. (G) Enrichment analysis for MDD-related genes. Negatively weighted genes were significantly enriched for genes associated with major depressive disorder by an independent genome wide association study (GWAS; (41)).

271 index, MI , a coefficient of the linear relationship between edgewise
 272 FC_{14} and FC_{14-26} at each node, was significantly more negative
 273 in females for cortical areas concentrated in the default mode net-
 274 work (DMN), ventral attentional and limbic networks, as well as
 275 subcortical nuclei.

276 The first explanatory hypothesis we considered was that the
 277 sex differences in developmental fMRI parameters were driven
 278 by sex differences in head motion during scanning. Males, espe-
 279 cially younger males, had more head movement than females. We
 280 addressed this potential confound by a two-stage pre-processing

281 pipeline which statistically corrected each participant's func-
 282 tional connectome for between-subject differences in head motion,
 283 indexed by framewise displacement (FD). These pre-processed
 284 data passed standard quality control criteria for movement-related
 285 effects on functional connectivity. Moreover, we repeated the entire
 286 analysis for male and female data separately, for a "motion-
 287 matched" subset of the data in which there was no significant sex
 288 difference in FD, and for all data after global signal regression.
 289 In all three sensitivity analyses, the key results of our prin-
 290 cipal analysis were qualitatively and quantitatively conserved. We

Sexually dimorphic development of depression-related brain networks during healthy human adolescence

291 therefore consider that head motion can be discounted as a sufficient explanation for sexual dimorphism in these developmental
292 parameters.

293 An alternative explanation is that sex differences in FC_{14-26} and MI reflect dimorphic development of specific cortico-
294 subcortical circuits. In particular, females had a more disruptive
295 pattern of adolescent development, indexed by negative ΔMI ,
296 whereby functional connections that were weak at 14 years became
297 stronger, and connections that were strong became weaker, over
298 the course of adolescence. We can interpret this as indicating sex
299 differences in an underlying process of reconfiguration or remodelling
300 of cortico-subcortical connectivity at a synaptic or neuronal scale.

301 To assess the plausibility of this biological interpretation, we
302 used pre-existing data on human brain gene expression, and the
303 dimension-reducing multivariate method of partial least squares
304 (PLS), to identify the set of genes that were most over- or under-
305 expressed in brain regions corresponding to the dimorphic system
306 defined by developmental fMRI. Enrichment analysis demon-
307 strated that the genes that were most strongly expressed in brain
308 regions with more disruptive development in females included sig-
309 nificantly more X chromosome genes than expected by chance.
310 The same set of genes was also significantly enriched for genes
311 that are known *a priori* to be expressed in cortical areas during
312 early (perinatal) development and in subcortical structures, such
313 as amygdala, during adolescent development.

314 Sexual differentiation of the brain has been proposed to occur
315 in two stages: an initial "organizational" stage before and imme-
316 diately after birth, and a later "activational" stage during ado-
317 lescent (47). It has long been argued that these events are driven
318 by gonadal hormones. However, more recent work suggests a com-
319 plex interplay of sex chromosomes and their downstream products
320 leading to sexual differentiation of brain cells (48; 49; 50). In
321 this context, the results of our enrichment analysis suggest that
322 cortical regions of the dimorphic fMRI system may become sexu-
323 ally differentiated during the early, organizational stage, whereas
324 inter-connected subcortical structures become differentiated dur-
325 ing the later, activational stage of development. In short, sexual
326 dimorphism of adolescent development of cortico-subcortical con-
327 nectivity could be driven by developmentally phased and sexually
328 dimorphic gene expression.

329 Finally, we assessed the pathogenic relevance of this dimorphi-
330 cally developing brain system to the greater risk of depression
331 in adolescent females. Macroscopically, the DMN and subcortical
332 structures that had more disruptive development in females, e.g.,
333 ventral medial prefrontal cortex, medial temporal gyrus, anterior
334 and posterior cingulate cortex, have previously been implicated
335 as substrates of depressive disorder (51; 52). This anatomical
336 convergence was quantified by the significant spatial correlation
337 between the whole brain map of sex differences in MI and an
338 independent map of MDD case-control differences in nodal degree
339 of functional connectivity. At a microscopic scale, the (PLS1)
340 list of genes transcriptionally co-located with the dimorphically
341 developing fMRI system were enriched for risk genes from prior
342 genome-wide association studies of MDD, as well as genes specifi-
343 cally expressed by adult neuronal and glial cells that have been
344 linked to neuroimaging phenotypes of depression (53). Psycholog-
345 ically, cognitive functions that typically activated the dimorphic

346 system, based on meta-analysis of a large prior database of task-
347 related fMRI studies, included reward-related processes that are
348 fundamental to the core depressive symptom of anhedonia.

Methodological issues

349 It is a strength of the study that our analysis of a dimorphi-
350 cally developing brain system is based on a longitudinal fMRI
351 dataset with approximately equal numbers of males and females
352 in each stratum of the adolescent age range. Head motion is known
353 to be a potentially problematic confound in developmental fMRI
354 (18; 19; 20). We have mitigated its impact on these data by a
355 two-step pre-processing pipeline that satisfied prior quality
356 control criteria; and we have demonstrated the robustness of our key
357 results to three alternative motion correction strategies, includ-
358 ing GSR (23) (SI Fig. S17-29). Limitations of the study include
359 our reliance on gene expression maps from post mortem exami-
360 nation of six adult, mostly male, brains. Biological validation of
361 this dimorphic fMRI system would be more directly informed by
362 sex-specific human brain maps of whole genome transcription in
363 adolescence. It will also be important in future to test the hypoth-
364 esis that an anatomically homologous cortico-subcortical system
365 has dimorphic adolescent development in animal models that allow
366 more precise but invasive analysis of the cellular and molecu-
367 lar substrates of fMRI phenotypes than is possible in humans.
368 We have shown that this normative developmental dimorphism is
369 anatomically, genetically and psychologically relevant to depres-
370 sion. However, further studies will be needed to test the hypothesis
371 that the emergence of depressive symptoms in adolescent females
372 is directly related to the dimorphically disruptive development of
373 DMN, limbic and subcortical connectivity that we have identified
374 in this cohort of healthy participants.

Conclusion

375 We conclude that there is sexual dimorphism in adolescent devel-
376 opment of functional connectivity between nodes of a human
377 cortico-subcortical system that is anatomically, genetically and
378 psychologically relevant to depression.

Methods

Study sample

384 Analysable fMRI data were available for $N=298$ healthy partici-
385 pants, aged 14 to 26 years, each scanned one to three times as part
386 of an accelerated longitudinal study of adolescent brain develop-
387 ment (Neuroscience in Psychiatry Network, NSPN; (37; 54; 6)).
388 Participants self-identified their sex as either male or female. There
389 were approximately equal numbers of males and females in each of
390 five age-defined strata at baseline (Table 1). All participants aged
391 16 years or older gave informed consent; participants younger than
392 16 gave informed assent and consent was provided by their parent
393 or guardian. The study was ethically approved by the National
394 Research Ethics Service and conducted in accordance with UK
395 National Health Service research governance standards.

398 *fMRI data acquisition*

399 Functional MRI data were acquired at three sites, on three identical 3T Siemens MRI scanners (Magnetom TIM Trio, VB17
400 software version), with a standard 32-channel radio-frequency
401 (RF) receive head coil and RF body coil for transmission using
402 a multi-echo echo-planar (ME-EPI) imaging sequence (55) with
403 the following scanning parameters: repetition time (TR): 2.42s;
404 GRAPPA with acceleration factor 2; Flip Angle: 90; matrix size:
405 64x64x34; FOV: 240x240mm; in-plane resolution: 3.75x3.75 mm;
406 slice thickness: 3.75 mm with 10% gap, sequential slice acquisition,
407 34 oblique slices; bandwidth 2368 Hz/pixel; echo times (TE) 13,
408 30.55 and 48.1 ms.

410 *fMRI data pre-processing*

411 Functional MRI data were preprocessed using multi-echo inde-
412 pendent component analysis (ME-ICA;(56; 57)) which identifies
413 and removes sources of variance in the times series that do not
414 scale linearly with TE and are therefore not representative of
415 the BOLD signal. Ventricular time series, representing variance in
416 cerebrospinal fluid (CSF), were regressed from parenchymal time
417 series using AFNI (58). Scans were parcellated into 360 bilateral
418 cortical regions using the Human Connectome Project (HCP; (59))
419 template and 16 bilateral sub-cortical regions (amygdala, caudate,
420 diencephalon, hippocampus, nucleus accumbens, pallidum, puta-
421 men, and thalamus) provided by Freesurfer (60). Regional time
422 series were averaged over all voxels within each parcel and band-
423 pass filtered by the discrete wavelet transform, corresponding to
424 frequency range 0.025-0.111 Hz (61).

425 After within-subject preprocessing and quality control, we
426 retained regional time series for 330 cortical and 16 subcorti-
427 cal nodes. Individual functional connectivity matrices $\{346 \times 346\}$
428 were estimated by Spearman's correlation for each possible pair
429 of nodes. Finally, we regressed each pairwise correlation or edge
430 on the time-averaged head motion of each participant (mean FD).
431 The residuals of this regression were the estimates of functional
432 connectivity used for further analysis (SI Fig. S2).

433 *Estimating parameters of adolescent development and testing sex
434 differences*

435 For males and females separately, we modeled region-wise and
436 edge-wise local cortico-cortico, subcortico-cortical and cortico-
437 subcortical (SI Fig. S3) maturational changes of functional con-
438 nectivity as a function of age, using linear mixed effects models
439 with fixed effects of age and site, and a subject-specific intercept
440 as a random effect.

441 Baseline connectivity (FC_{14}) was estimated as the predicted
442 FC at age 14, the adolescent rate of change (FC_{14-26}) as the slope
443 of the model (Fig. 1). We calculated the maturational index (MI),
444 as the Spearman correlation of edge-wise FC_{14} and FC_{14-26} (Fig.
445 2).

446 We parametrically tested for the significance of the sex dif-
447 ference in MI in a Z -test of the equivalence of the slopes of the
448 regression of FC_{14} on FC_{14-26} for males and females (62).

449 *Enrichment analysis*

450 We extracted the first component (PLS1) of a partial least squares
451 regression of ΔMI on post mortem gene expression data from the

Allen Human Brain Atlas collected from 6 donor brains (5 males)
452 (27) (Fig. 4). We then used a median rank-based approach to
453 assess the enrichment of PLS1 on several published gene lists (63).
454 This approach estimates the degree to which the spatial expres-
455 sion of PLS1 genes is related to a given gene set by comparing the
456 observed (PLS1) median gene rank to a null distribution of median
457 ranks from genes that were randomly sampled from the PLS com-
458 ponent and matched by gene length (for null models, refer to SI
459 Fig. S4-7). Thus if a gene set's real median rank is significantly
460 lower than expected by chance the gene set is associated with the
461 bottom of PLS1 and if it is higher, its genes are enriched towards
462 the top end of the component.

463 *fMRI connectivity in major depressive disorder*

464 We constructed a MDD case-control map by conducting multiple
465 t -tests for the difference in nodal weighted degree of functional
466 connectivity between two groups of resting state fMRI data from
467 an independent sample of 47 healthy controls and 87 MDD cases
468 (SI Text, SI Table S3). We then correlated the ΔMI map with
469 the MDD case-control t map (Fig. 3).

470 *Data and code availability*

471 The main data set used for our analysis will be made publicly
472 accessible upon publication. The code can be found at https://github.com/LenaDorfSchmidt/sex_differences_adolescence.git.

473 *Acknowledgements*

474 We appreciate Dr Varun Warrier's advice on statistical meth-
475 ods for gene set enrichment analyses. This study was funded
476 by a collaborative award from the Wellcome Trust for the Neu-
477 roscience in Psychiatry Network at University College London
478 and the University of Cambridge. Additional funding was pro-
479 vided by the NIHR Cambridge Biomedical Research Centre.
480 EB is an NIHR Senior Investigator. LD was supported by the
481 Gates Cambridge Trust. P.E.V. is a Fellow of MQ: Transform-
482 ing Metal Health (MQF1724) and of the Alan Turing Institute
483 funded by EPSRC grant EP/N510129/1. R.A.I.B. was supported
484 by a British Academy Post-Doctoral fellowship and the Autism
485 Research Trust. S.E.M. was funded by a Fellowship from The
486 Alan Turing Institute, London and a Henslow Fellowship at Lucy
487 Cavendish College, University of Cambridge, funded by the Cam-
488 bridge Philosophical Society. Data were curated and analysed
489 using a computational facility funded by an MRC research infra-
490 structure award (MR/M009041/1) and supported by the NIHR
491 Cambridge Biomedical Research Centre. This research was co-
492 funded by the NIHR Cambridge Biomedical Research Centre. The
493 views expressed are those of the authors and not necessarily those
494 of the NHS, the NIHR or the Department of Health and Social
495 Care.

496 *Conflict of interest*

497 E.T.B. serves on the Scientific Advisory Board of Sosei Heptares.

498 *Author Contributions*

499 L.D., P.E.V., and E.T.B. designed research. L.D., R.A.I.B., and
500 J.S. analyzed data. L.D., R.R.-G, F.V., M.G.K., P.E.V. performed

503 research. J.S., R.A.I.B, S.E.M., M.G.B., and A.A. contributed
504 new reagents/analytical tools. S.R.W. advised on statistical meth-
505 ods E.T.B., P.J., R.D., I.G., and P.F. designed the NSPN study.
506 N.A.H. designed the Biodep study E.T.B. and L.D. wrote the
507 paper.

508 509 References

510 1 Elizabeth R. Sowell, Paul M. Thompson, and Arthur W. Toga. Mapping
511 changes in the human cortex throughout the span of life. *The*
512 *Neuroscientist*, 10(4):372–392, 2004. PMID: 15271264.

513 2 J.N. Giedd. Structural magnetic resonance imaging of the adolescent
514 brain. *Annals of the New York Academy of Sciences*, 1021(1):77–85,
515 2004.

516 3 A. Raznahan, J. P. Lerch, N. Lee, D. Greenstein, G. L. Wallace,
517 M. Stockman, L. Clasen, P. W. Shaw, and J. N Giedd. Patterns
518 of coordinated anatomical change in human cortical development: a
519 longitudinal neuroimaging study of maturational coupling. *Neuron*,
520 72(5):873–884, 2011.

521 4 František Váša, Jakob Seidlitz, Rafael Romero-Garcia, Kirstie J
522 Whitaker, Gideon Rosenthal, Petra E Vértes, Maxwell Shinn, Aaron
523 Alexander-Bloch, Peter Fonagy, Raymond J Dolan, Peter B Jones,
524 Ian M Goodyer, Olaf Sporns, and Edward T Bullmore. Adolescent
525 Tuning of Association Cortex in Human Structural Brain Networks.
526 *Cerebral Cortex*, 28(1):281–294, jan 2018.

527 5 Petra E. Vértes, Timothy Rittman, Kirstie J. Whitaker, Rafael
528 Romero-Garcia, František Váša, Manfred G. Kitzbichler, Konrad
529 Wagstyl, Peter Fonagy, Raymond J. Dolan, Peter B. Jones, Ian M.
530 Goodyer, null null, and Edward T. Bullmore. Gene transcription
531 profiles associated with inter-modular hubs and connection distance
532 in human functional magnetic resonance imaging networks. *Philosophical
533 Transactions of the Royal Society B: Biological Sciences*,
534 371(1705):20150362, 2016.

535 6 František Váša, Rafael Romero-Garcia, Manfred G. Kitzbichler,
536 Jakob Seidlitz, Kirstie J. Whitaker, Matilde M. Vaghi, Prantik
537 Kundu, Ameera X. Patel, Peter Fonagy, Raymond J. Dolan, Peter B.
538 Jones, Ian M. Goodyer, Petra E. Vértes, and Edward T. Bullmore.
539 Conservative and disruptive modes of adolescent change in human
540 brain functional connectivity. *Proceedings of the National Academy
541 of Sciences*, 117(6):3248–3253, 2020.

542 7 Carlo Faravelli, Maria Alessandra Scarpati, Giovanni Castellini, and
543 Carolina Lo Sauro. Gender differences in depression and anxiety: The
544 role of age. *Psychiatry Research*, 210(3):1301–1303, dec 2013.

545 8 Jill M. Cyranowski, Ellen Frank, Elizabeth Young, and M. Katherine
546 Shear. Adolescent Onset of the Gender Difference in Lifetime Rates
547 of Major Depression. *Archives of General Psychiatry*, 57(1):21, jan
548 2000.

549 9 Benjamin L. Hankin, Lyn Y. Abramson, Terrie E. Moffitt, Phil A.
550 Silva, Rob McGee, and Kathryn E. Angell. Development of depression
551 from preadolescence to young adulthood: Emerging gender
552 differences in a 10-year longitudinal study. *Journal of Abnormal
553 Psychology*, 107(1):128–140, 1998.

554 10 Tomáš Paus, Matcheri Keshavan, and Jay N. Giedd. Why do many
555 psychiatric disorders emerge during adolescence? *Nature Reviews
556 Neuroscience*, 9(12):947–957, dec 2008.

557 11 Bharat Biswal, F. Zerrin Yetkin, Victor M. Haughton, and James S.
558 Hyde. Functional connectivity in the motor cortex of resting human
559 brain using echo-planar mri. *Magnetic Resonance in Medicine*,
560 34(4):537–541, oct 1995.

561 12 Alex Fornito, Andrew Zalesky, and Edward T. Bullmore. *Funda-
562 mentals of brain network analysis / Alex Fornito, Andrew Zalesky,
563 Edward T. Bullmore*. Elsevier/Academic Press Amsterdam ; Boston,
564 2016.

565 13 Damien A. Fair, Alexander L. Cohen, Jonathan D. Power, Nico U. F.
566 Dosenbach, Jessica A. Church, Francis M. Miezin, Bradley L. Schlag-
567 gar, and Steven E. Petersen. Functional Brain Networks Develop
568 from a “Local to Distributed” Organization. *PLoS Computational
569 Biology*, 5(5):e1000381, may 2009.

570 14 D. A. Fair, N. U. F. Dosenbach, J. A. Church, A. L. Cohen,
571 S. Brahmhett, F. M. Miezin, D. M. Barch, M. E. Raichle, S. E.
572 Petersen, and B. L. Schlaggar. Development of distinct control
573 networks through segregation and integration. *Proceedings of the
574 National Academy of Sciences*, 104(33):13507–13512, aug 2007.

575 15 Nico U. F. Dosenbach, Binyam Nardos, Alexander L. Cohen,
576 Damien A. Fair, Jonathan D. Power, Jessica A. Church, Steven M.
577 Nelson, Gagan S. Wig, Alecia C. Vogel, Christina N. Lessov-
578 Schlaggar, Kelly Anne Barnes, Joseph W. Dubis, Eric Feczkó,
579 Rebecca S. Coalson, John R. Pruett, Deanna M. Barch, Steven E.
580 Petersen, and Bradley L. Schlaggar. Prediction of Individual Brain
581 Maturity Using fMRI. *Science*, 329(5997):1358–1361, sep 2010.

582 16 Kirstie J Whitaker, Petra E Vértes, Rafael Romero-Garcia,
583 František Váša, Michael Moutoussis, Gita Prabhu, Nikolaus
584 Weiskopf, Martina F Callaghan, Konrad Wagstyl, Timothy Rittman,
585 Roger Tait, Cinly Ooi, John Suckling, Becky Inkster, Peter Fonagy,
586 Raymond J Dolan, Peter B Jones, Ian M Goodyer, the NSPN NSPN
587 Consortium, and Edward T Bullmore. Adolescence is associated with
588 genetically patterned consolidation of the hubs of the human brain
589 connectome. *Proceedings of the National Academy of Sciences of the
590 United States of America*, 113(32):9105–10, aug 2016.

591 17 Kathryn L. Mills, Anne-Lise Goddings, Liv S. Clasen, Jay N.
592 Giedd, and Sarah-Jayne Blakemore. The Developmental Mismatch
593 in Structural Brain Maturation during Adolescence. *Developmental
594 Neuroscience*, 36(3-4):147–160, 2014.

595 18 Jonathan D Power, Kelly A Barnes, Abraham Z Snyder, Bradley L
596 Schlaggar, and Steven E Petersen. Spurious but systematic corre-
597 lations in functional connectivity MRI networks arise from subject
598 motion. *NeuroImage*, 59(3):2142–54, feb 2012.

599 19 Theodore D. Satterthwaite, Daniel H. Wolf, James Loughead,
600 Kosha Ruparel, Mark A. Elliott, Hakon Hakonarson, Ruben C. Gur,
601 and Raquel E. Gur. Impact of in-scanner head motion on multi-
602 ple measures of functional connectivity: Relevance for studies of
603 neurodevelopment in youth. *NeuroImage*, 60(1):623 – 632, 2012.

604 20 Theodore D. Satterthwaite, Daniel H. Wolf, Kosha Ruparel, Guray
605 Eruç, Mark A. Elliott, Simon B. Eickhoff, Efstatios D. Gen-
606 natas, Chad Jackson, Karthik Prabhakaran, Alex Smith, Hakon
607 Hakonarson, Ragini Verma, Christos Davatzikos, Raquel E. Gur,
608 and Ruben C. Gur. Heterogeneous impact of motion on fundamental
609 patterns of developmental changes in functional connectivity during
610 youth. *NeuroImage*, 83:45 – 57, 2013.

611 21 Jonathan D. Power, Mark Plitt, Stephen J. Gotts, Prantik Kundu,
612 Valerie Voon, Peter A. Bandettini, and Alex Martin. Ridding fmri
613 data of motion-related influences: Removal of signals with distinct
614 spatial and physical bases in multiecho data. *Proceedings of the
615 National Academy of Sciences*, 115(9):E2105–E2114, 2018.

616 22 Birn R. M. Handwerker D. A. Jones T. B. Bandettini P. A. Mur-
617 phy, K. The impact of global signal regression on resting state
618 correlations: are anti-correlated networks introduced? *NeuroImage*,
619 44(3):893–905, 2009.

620 23 Marieke L. Schölvink, Alexander Maier, Frank Q. Ye, Jeff H.
621 Duyn, and David A. Leopold. Neural basis of global resting-state

622 fmri activity. *Proceedings of the National Academy of Sciences*,
623 107(22):10238–10243, 2010.

624 **24** Schweizer TA, Graham SJ, Maknojia S, Churchill NW. Resting state
625 fmri: Going through the motions. *Front Neurosci*, 13(825), 2019.

626 **25** Massimo Filippi, Paola Valsasina, Paolo Misci, Andrea Falini, Gian-
627 carlo Comi, and Maria A. Rocca. The organization of intrinsic brain
628 activity differs between genders: A resting-state fMRI study in a
629 large cohort of young healthy subjects. *Human Brain Mapping*,
630 34(6):1330–1343, jun 2013.

631 **26** D Tomasi and N D Volkow. Aging and functional brain networks.
632 *Molecular Psychiatry*, 17(5):549–558, may 2012.

633 **27** Elena A Allen, Erik B Erhardt, Eswar Damaraju, William
634 Gruner, Judith M Segall, Rogers F Silva, Martin Havlicek, Srinivas
635 Rachakonda, Jill Fries, Ravi Kalyanam, Andrew M Michael,
636 Arvind Caprihan, Jessica A Turner, Tom Eichele, Steven Adelsheim,
637 Angela D Bryan, Juan Bustillo, Vincent P Clark, Sarah W Feldstein
638 Ewing, Francesca Filbey, Corey C Ford, Kent Hutchison, Rex E Jung,
639 Kent A Kiehl, Piyadasa Kodituwakk, Yuko M Komesu, Andrew R
640 Mayer, Godfrey D Pearlson, John P Phillips, Joseph R Sadek,
641 Michael Stevens, Ursina Teuscher, Robert J Thoma, and Vince D
642 Calhoun. A baseline for the multivariate comparison of resting-state
643 networks. *Frontiers in systems neuroscience*, 5:2, 2011.

644 **28** Bharat B Biswal, Maarten Mennes, Xi-Nian Zuo, Suril Gohel, Clare
645 Kelly, Steve M Smith, Christian F Beckmann, Jonathan S Adel-
646 stein, Randy L Buckner, Stan Colcombe, Anne-Marie Dogonowski,
647 Monique Ernst, Damien Fair, Michelle Hampson, Matthew J Hopt-
648 man, James S Hyde, Vesa J Kiviniemi, Rolf Kötter, Shi-Jiang Li,
649 Ching-Po Lin, Mark J Lowe, Clare Mackay, David J Madden, Kristof-
650 fer H Madsen, Daniel S Margulies, Helen S Mayberg, Katie McMa-
651 hon, Christopher S Monk, Stewart H Mostofsky, Bonnie J Nagel,
652 James J Pekar, Scott J Peltier, Steven E Petersen, Valentin Riedl,
653 Serge A R B Rombouts, Bart Rypma, Bradley L Schlaggar, Sein
654 Schmidt, Rachael D Seidler, Greg J Siegle, Christian Sorg, Gao-Jun
655 Teng, Juha Veijola, Arno Villringer, Martin Walter, Lihong Wang,
656 Xu-Chu Weng, Susan Whitfield-Gabrieli, Peter Williamson, Chris-
657 tian Windischberger, Yu-Feng Zang, Hong-Ying Zhang, F Xavier
658 Castellanos, and Michael P Milham. Toward discovery science of
659 human brain function. *Proceedings of the National Academy of
660 Sciences of the United States of America*, 107(10):4734–9, mar 2010.

661 **29** Robyn L. Bluhm, Elizabeth A. Osuch, Ruth A. Lanius, Kris-
662 tine Boksman, Richard W.J. Neufeld, Jean Théberge, and Peter
663 Williamson. Default mode network connectivity: effects of age, sex,
664 and analytic approach. *NeuroReport*, 19(8):887–891, may 2008.

665 **30** Dustin Scheinost, Emily S. Finn, Fuyuze Tokoglu, Xilin Shen,
666 Xenophon Papademetris, Michelle Hampson, and R. Todd Consta-
667 ble. Sex differences in normal age trajectories of functional brain
668 networks. *Human Brain Mapping*, 36(4):1524–1535, apr 2015.

669 **31** Irit Weissman-Fogel, Massieh Moayedi, Keri S. Taylor, Geoff Pope,
670 and Karen D. Davis. Cognitive and default-mode resting state net-
671 works: Do male and female brains “rest” differently? *Human Brain
672 Mapping*, 31(11):n/a–n/a, mar 2010.

673 **32** Gabriela Alarcón, Anita Cservenka, Marc D. Rudolph, Damien A.
674 Fair, and Bonnie J. Nagel. Developmental sex differences in resting
675 state functional connectivity of amygdala sub-regions. *NeuroImage*,
676 115:235–244, jul 2015.

677 **33** L.A. Kilpatrick, D.H. Zald, J.V. Pardo, and L.F. Cahill. Sex-
678 related differences in amygdala functional connectivity during resting
679 conditions. *NeuroImage*, 30(2):452–461, apr 2006.

680 **34** Chao Zhang, Nathan D. Cahill, Mohammad R. Arbabshirani, Tonya
681 White, Stefi A. Baum, and Andrew M. Michael. Sex and Age Effects
682 of Functional Connectivity in Early Adulthood. *Brain Connectivity*,
683 6(9):700–713, nov 2016.

684 **35** Chao Zhang, Chase C. Dougherty, Stefi A. Baum, Tonya White,
685 and Andrew M. Michael. Functional connectivity predicts gender:
686 Evidence for gender differences in resting brain connectivity. *Human
687 Brain Mapping*, 39(4):1765–1776, apr 2018.

688 **36** R Casanova, C T Whitlow, B Wagner, M A Espeland, and J A
689 Maldjian. Combining graph and machine learning methods to ana-
690 lyze differences in functional connectivity across sex. *The open
691 neuroimaging journal*, 6:1–9, 2012.

692 **37** Beatrix Kiddle, Becky Inkster, Gita Prabhu, Michael Moutous-
693 sis, Kirstie J Whitaker, Edward T Bullmore, Raymond J Dolan,
694 Peter Fonagy, Ian M Goodyer, and Peter B Jones. Cohort Profile:
695 The NSPN 2400 Cohort: a developmental sample supporting the
696 Wellcome Trust NeuroScience in Psychiatry Network. *International
697 Journal of Epidemiology*, 47(1):18–19g, 11 2017.

698 **38** Ameera X. Patel, Prantik Kundu, Mikail Rubinov, P. Simon Jones,
699 Petra E. Vértes, Karen D. Ersche, John Suckling, and Edward T.
700 Bullmore. A wavelet method for modeling and despiking motion arti-
701 facts from resting-state fMRI time series. *NeuroImage*, 95:287–304,
702 jul 2014.

703 **39** Krienen F. M. Sepulcre J. Sabuncu M. R. Lashkari D. Hollinshead
704 M. Roffman J. L. Smoller J. W. Zöllei L. Polimeni J. R. Fischl B. Liu
705 H. Buckner R. L. year = 2011 title = The organization of the human
706 cerebral cortex estimated by intrinsic functional connectivity journal
707 = Journal of neurophysiology volume = 106 number = 3 pages =
708 1125–1165 doi = <https://doi.org/10.1152/jn.00338.2011> Yeo, B. T.

709 **40** Poldrack R. A. Nichols T. E. Van Essen D. C. Wager T. D.
710 Yarkoni, T. Large-scale automated synthesis of human functional
711 neuroimaging data. *Nature methods*, 8(8):665–670, 2011.

712 **41** D.M. Howard, M.J. Adams, M. Shirali, T.K. Clarke, R.E. Marioni,
713 G. Davies, J.R.I. Coleman, C. Alloza, X. Shen, M.C. Barbu, E.M.
714 Wigmore, J. Gibson, 23andMe Research Team, S.P. Hagenaars, C.M.
715 Lewis, J. Ward, D.J. Smith, P.F. Sullivan, C.S. Haley, G. Breen,
716 I.J. Deary, and A.M. McIntosh. Genome-wide association study of
717 depression phenotypes in uk biobank identifies variants in excitatory
718 synaptic pathways. *Nature Communications*, 9(1470), 2018.

719 **42** Sarah E Morgan, Jakob Seidlitz, Kirstie J Whitaker, Rafael
720 Romero-Garcia, Nicholas E Clifton, Cristina Scarpazza, Therese van
721 Amelsvoort, Machteld Marcelis, Jim van Os, Gary Donohoe, David
722 Mothersill, Aiden Corvin, Andrew Pocklington, Armin Raznahan,
723 Philip McGuire, Petra E Vértes, and Edward T Bullmore. Cortical
724 patterning of abnormal morphometric similarity in psychosis is
725 associated with brain expression of schizophrenia-related genes. *Pro-
726 ceedings of the National Academy of Sciences of the United States
727 of America*, 116(19):9604–9609, may 2019.

728 **43** Ying Zhu, André M. M. Sousa, Tianliuyun Gao, Mario Skarica,
729 Mingfeng Li, Gabriel Santpere, Paula Esteller-Cucala, David Juan,
730 Luis Ferrández-Peral, Forrest O. Gulden, Mo Yang, Daniel J. Miller,
731 Tomas Marques-Bonet, Yuka Imamura Kawasawa, Hongyu Zhao,
732 and Nenad Sestan. Spatiotemporal transcriptomic divergence across
733 human and macaque brain development. *Science*, 362(6420), 2018.

734 **44** Xiaoxiao Xu, Alan B. Wells, David R. O'Brien, Arye Nehorai, and
735 Joseph D. Dougherty. Cell type-specific expression analysis to iden-
736 tify putative cellular mechanisms for neurogenetic disorders. *Journal
737 of Neuroscience*, 34(4):1420–1431, 2014.

738 **45** B. Lake, S. Chen, B. Sos, J. Fan, G.E. Kaeser, Y.C. Yung, T.E.
739 Duong, D. Gao, J. Chun, Kharchenko, and K. P.V., Zhang. Integrative
740 single-cell analysis of transcriptional and epigenetic states in the
741 human adult brain. *Nature Biotechnology*, 36:70–80, 2018.

742 46 Damon Polioudakis, Luis [de la Torre-Ubieta], Justin Langerman, 802
743 Andrew G. Elkins, Xu Shi, Jason L. Stein, Celine K. Vuong, 803
744 Susanne Nichterwitz, Melinda Gevorgian, Carli K. Opland, 804
745 Daniel Lu, William Connell, Elizabeth K. Ruzzo, Jennifer K. Lowe, 805
746 Tarik Hadzic, Flora I. Hinz, Shan Sabri, William E. Lowry, Mark B. 806
747 Gerstein, Kathrin Plath, and Daniel H. Geschwind. A single-cell 807
748 transcriptomic atlas of human neocortical development during 808
749 mid-gestation. *Neuron*, 103(5):785 – 801.e8, 2019. 809

750 47 Charles H. Phoenix, Robert W. Goy, Arnold A. Gerall, and 810
751 William C. Young. Organizing action of prenatally administered 811
752 testosterone propionate on the tissue mediating mating behavior in 812
753 the female guinea pig. *Endocrinology*, 65(3):369–382, 09 1959. 813

754 48 Laura Carruth, Ingrid Reisert, and Arthur Arnold. Sex 814
755 chromosome genes directly affect brain sexual differentiation. *Nature 815
756 neuroscience*, 5:933–4, 11 2002. 816

757 49 Arthur P. Arnold, Jun Xu, William Grisham, Xuqi Chen, Yong- 817
758 Hwan Kim, and Yuichiro Itoh. Minireview: Sex Chromosomes and 818
759 Brain Sexual Differentiation. *Endocrinology*, 145(3):1057–1062, 03 819
760 2004. 820

761 50 Margaret M McCarthy and Arthur P Arnold. Reframing sexual 821
762 differentiation of the brain. *Nature neuroscience*, 14(6):677–83, 2011. 822

763 51 Kathryn R. Cullen, Dylan G. Gee, Bonnie Klimes-Dougan, Vilma 823
764 Gabbay, Leslie Hulvershorn, Bryon A. Mueller, Jazmin Camchong, 824
765 Christopher J. Bell, Alaa Houri, Sanjiv Kumra, Kelvin O. Lim, 825
766 F. Xavier Castellanos, and Michael P. Milham. A preliminary 826
767 study of functional connectivity in comorbid adolescent depression. 827
768 *Neuroscience Letters*, 460(3):227–231, sep 2009. 828

769 52 Colm G. Connolly, Jing Wu, Tiffany C. Ho, Fumiko Hoeft, Owen 829
770 Wolkowitz, Stuart Eisendrath, Guido Frank, Robert Hendren, Jeffrey 830
771 E. Max, Martin P. Paulus, Susan F. Tapert, Dipavo Banerjee, 831
772 Alan N. Simmons, and Tony T. Yang. Resting-State Functional 832
773 Connectivity of Subgenual Anterior Cingulate Cortex in Depressed 833
774 Adolescents. *Biological Psychiatry*, 74(12):898–907, dec 2013. 834

775 53 Kevin M Anderson, Meghan A Collins, Ru Kong, Kacey Fang, Jing- 835
776 wei Li, Tong He, Adam M Chekroud, B.T. Thomas Yeo, and Avram J 836
777 Holmes. Convergent molecular, cellular, and neural signatures of 837
778 major depressive disorder. *bioRxiv*, 2020. 838

779 54 Kirstie J Whitaker, Petra E Vértes, Rafael Romero-Garcia, 839
780 František Váša, Michael Moutoussis, Gita Prabhu, Nikolaus 840
781 Weiskopf, Martina F Callaghan, Konrad Wagstyl, Timothy Rittman, 841
782 Roger Tait, Cinyi Ooi, John Suckling, Becky Inkster, Peter Fonagy, 842
783 Raymond J Dolan, Peter B Jones, Ian M Goodyer, the NSPN NSPN 843
784 Consortium, and Edward T Bullmore. Adolescence is associated with 844
785 genetically patterned consolidation of the hubs of the human brain 845
786 connectome. *Proceedings of the National Academy of Sciences of the 846
787 United States of America*, 113(32):9105–10, aug 2016. 847

788 55 Markus Barth, Jürgen R Reichenbach, Ramesh Venkatesan, Ewald 848
789 Moser, and E. Mark Haacke. High-resolution, multiple gradient-echo 849
790 functional MRI at 1.5 T. *Magnetic Resonance Imaging*, 17(3):321– 850
791 329, apr 1999. 851

792 56 Prantik Kundu, Souheil J. Inati, Jennifer W. Evans, Wen-Ming 852
793 Luh, and Peter A. Bandettini. Differentiating BOLD and non-BOLD 853
794 signals in fMRI time series using multi-echo EPI. *NeuroImage*, 854
795 60(3):1759–1770, apr 2012. 855

796 57 Prantik Kundu, Noah D Brenowitz, Valerie Voon, Yulia Worbe, 856
797 Petra E Vértes, Souheil J Inati, Ziad S Saad, Peter A Bandettini, 857
798 and Edward T Bullmore. Integrated strategy for improving func- 858
799 tional connectivity mapping using multiecho fMRI. *Proceedings of 860
800 the National Academy of Sciences of the United States of America*, 861
801 110(40):16187–92, oct 2013. 862

58 Robert W. Cox. AFNI: Software for Analysis and Visualization 802
of Functional Magnetic Resonance Neuroimages. *Computers and 803
Biomedical Research*, 29(3):162–173, jun 1996. 804

59 Matthew F. Glasser, Timothy S. Coalson, Emma C. Robinson, 805
Carl D. Hacker, John Harwell, Essa Yacoub, Kamil Ugurbil, Jesper 806
Andersson, Christian F. Beckmann, Mark Jenkinson, Stephen M. 807
Smith, and David C. Van Essen. A multi-modal parcellation of 808
human cerebral cortex. *Nature*, 536(7615):171–178, aug 2016. 809

60 P. A. Filipek, C. Richelme, D. N. Kennedy, and V. S. Caviness. The 810
Young Adult Human Brain: An MRI-based Morphometric Analysis. 811
Cerebral Cortex, 4(4):344–360, jul 1994. 812

61 Ed Bullmore, Jalal Fadili, Voichita Maxim, Levent Şendur, Brandon 813
Whitcher, John Suckling, Michael Brammer, and Michael Breakspear. 814
Wavelets and functional magnetic resonance imaging of the 815
human brain. *NeuroImage*, 23:S234–S249, jan 2004. 816

62 Raymond Paternoster, Robert Brame, Paul Mazerolle, and Alex 817
Piquero. Using the Correct Statistical Test for the Equality of 818
Regression Coefficients. *Criminology*, 36(4):859–866, nov 1998. 819

63 Jakob Seidlitz, Ajay Nadig, Siyuan Liu, Richard A.I. Bethlehem, 820
Petra E. Vértes, Sarah E. Morgan, František Váša, Rafael 821
Romero-Garcia, François M. Lalonde, Liv S. Clasen, Jonathan D. 822
Blumenthal, Casey Paquola, Boris Bernhardt, Konrad Wagstyl, 823
Damon Polioudakis, Luis de la Torre-Ubieta, Daniel H. Geschwind, 824
Joan C. Han, Nancy R. Lee, Declan G. Murphy, Edward T. Bull- 825
more, and Armin Raznahan. Transcriptomic and cellular decoding 826
of regional brain vulnerability to neurogenetic disorders. *Nature 827
Communications*, 11(3358), 2020. 828